

Hopf bifurcation at the phase-locking point of an externally driven, homogeneously broadened laser

R. C. Buceta

Departamento de Física, Facultad de Ciencias Exactas y Naturales, Universidad Nacional de Mar del Plata, Funes 3350 (7600) Mar del Plata, Argentina

M. S. Torre and H. F. Ranea-Sandoval*

Instituto de Física "Arroyo Seco," Facultad de Ciencias Exactas, Universidad Nacional del Centro de la Provincia de Buenos Aires, Pinto 399 (7000) Tandil, Buenos Aires, Argentina
(Received 9 September 1992)

A model describing the dynamics of a white- and colored-noise injected-signal, single-mode, homogeneously broadened laser in the semiclassical limit is presented. The system has a Hopf bifurcation above the threshold where phase locking occurs. This bifurcation point is characterized by a simple relation between gain and loss parameters, detuning, and external-driving-field intensity. The stochastic normal form of the system near the bifurcation point is found and the contribution of the harmonics of the bifurcation frequency in the spectrum is thus, analytically determined. As a result of gain saturation and phase-excursion phenomena, the resonances become apparent before reaching the bifurcation point for low driving-force values. Above this bifurcation point, the spectrum is that of a frequency-locked laser in the presence of noise. These results are consistent with numerical experiments carried out with both white and colored noise. In the case of colored noise, resonances are wider than in the white-noise case, depending on the correlation time of the multiplicative and the additive terms into which noise has been decomposed.

PACS number(s): 42.50.Ar, 42.55.-f, 05.40.+j, 42.60.Mi

I. INTRODUCTION

Since the phenomena of frequency locking and linewidth narrowing in lasers have first been reported in external cavity seeding, the response of a nonlinear system to an external coherent injection has been the subject of numerous publications. A number of workers have developed the theory of injection locking [1] of lasers which was later followed by studies on phased arrays of lasers [2, 3]. The Langevin equation has been used to account for additive, white noise present in the system. Noise in the driving force has been taken as a dominant factor in bidirectional ring-gyroscope-type lasers, where the backscattering of one mode acts as a seed for the counterpropagating mode, locking them in phase [4]. Moreover, externally driven laser systems have shown chaotic behaviors [5, 6], noise having been considered as very important in bifurcation cascades, because it can drive the system away from an instability, thus blocking the route to chaos.

The problem of nonlinear systems driven by stochastic forces at a bifurcation point is also of interest in nonequilibrium statistical physics. Starting from the works by Kapitaniak [7], many attempts have been made to study the distributions of oscillators under such conditions. In the last few years, both white and colored noise (Ornstein-Uhlenbeck processes) have been deeply studied in nonlinear oscillators [8, 9], and retarded-field effects were compared to a special type of colored noise [10]. On the other hand, noise in the vicinity of a bifurcation or near an instability point has long been considered as a source for interesting results for statistical

physics as well as in laser theory [11–15]. The quantum noise can also be modeled by a Langevin equation, as has been used by Aguado and San Miguel in an analysis of a molecular-dye-laser operation [16].

In this paper we present the stationary solutions for a two-level, homogeneously broadened, single-frequency laser with injected signal, in the semiclassical, slowly-varying-amplitude and phase approximation. It is a well known fact [17] that homogeneously broadened lasers, working in the vicinity of the threshold, can be modeled by the Hopf stochastic normal form for the electric field in the cavity. Starting from these ideas, we prove that it is possible to construct, for an arbitrary driving force, a stochastic normal form equation which qualitatively shows the main features of the power spectral density.

We describe first a deterministic model in which we have found that, at certain operating conditions, the system will reach a bifurcation point characterized by the internal as well as by the external parameters, i.e., the gain, the loss per pass, the amplitude of the driving force, and the detuning between the laser and the external injected signal. This bifurcation is a Hopf-type bifurcation as it is analyzed below. First, the analysis is performed dealing with the stability of the solutions of the deterministic model. Secondly, we introduce noise in the relevant parameters of the system, i.e., in the frequency and in the amplitude of the injected field. The first is a multiplicative noise and the second an additive one. We present here the case where these parameters fluctuate with well defined mean values. This instance includes an analysis of colored noise which satisfies an Ornstein-Uhlenbeck process, where the corresponding white-noise

limit is reached for zero correlation time. The effects of the memory of the process are a shift in the system frequency and a broadening of the peaks of its harmonics near the bifurcation point.

Finally, several examples were inspected by numerical simulation of the model and it is shown that the dominant peak contributions to the power spectral density are consistent with the theory. Our approach allows us to extend the analysis to driving injection amplitudes, not necessarily weak, a fact that is responsible for the spectral shift of the fundamental frequency and its harmonics.

II. DETERMINISTIC MODEL

Let us consider a single-frequency, homogeneously broadened, injected-signal laser. In order to avoid hole burning effects due to counterpropagating waves through the gain medium, and to decouple the oscillator and the slave laser, it is convenient to model the laser as a *one-way* ring cavity.

The mode amplitude inside the cavity is described by a complex differential equation for the electric field in the rotating-wave approximation

$$\dot{\mathcal{E}} = [i\Delta\nu + G(E)]\mathcal{E} + \Delta_c\sqrt{T}E_I, \quad (1)$$

where $\mathcal{E} = E(t)e^{i\theta(t)}$ is the laser field with a phase $\theta(t) = \phi_L(t) - \phi_I(t)$, $\phi_L(t)$, $\phi_I(t)$ being the phase of the laser and $\phi_I(t)$ the injected field phase. The operating frequency of the laser is $\nu_L = \nu_I + d\phi_L/dt$. The detuning between both lasers is $\Delta\nu = \nu_L - \nu_I$. The injected signal outside the cavity is described by a field $\mathcal{E}_I(t) = E_I(t)e^{i\nu_I t}$; Δ_c is the free spectral range of the laser cavity and T the transmission coefficient of the coupling mirror. Finally, $G(E) = -K + \Gamma/(1 + E^2)$ is the saturated net gain, where K is the loss rate and Γ the small signal gain.

In the case of nonresonant injection ($\Delta\nu \neq 0$), a suitable time scaling ($\tau = \Delta\nu t$) yields

$$\partial_\tau \mathcal{E} = [i + g(E)]\mathcal{E} + F, \quad (2)$$

where

$$g(E) = \frac{G(E)}{\Delta\nu} = -\kappa + \frac{\gamma}{1 + E^2}, \quad (3)$$

and

$$F = \frac{\Delta_c\sqrt{T}E_I}{\Delta\nu}.$$

In the case $F = 0$, the power spectral density will consist in a single frequency at ν_L , as is readily seen considering $\Delta\nu = \nu_L$.

III. STATIONARY SOLUTIONS: STABILITY AND BIFURCATION POINT

We will now determine the stability of the stationary-state solutions of Eq. (2) near the bifurcation point, and the eigenvalues defining the bifurcation point of the system.

Let $\mathcal{E}_s = X_s + iY_s$ be the stationary-state field such that

$$(i + g_s)\mathcal{E}_s + F = 0, \quad (4)$$

where $g_s = g_s(E)$ is the stationary net gain. The solutions for the amplitude and the phase satisfy the transcendental equations,

$$E_s^2 = \frac{\delta - g_s}{\kappa + g_s}, \quad (5)$$

$$\varphi_s = -\cot^{-1} g_s,$$

where $\delta = \gamma - \kappa$ is the adimensional small signal net gain parameter, and

$$g_s = -\frac{X_s}{Y_s}. \quad (6)$$

Equations (5) define the solution curve of possible stationary states for the electric field.

For κ and γ fixed, the solution curve for Eqs. (5) is independent of F . Considering its intersection with the curve

$$F \sin \varphi_s = E_s, \quad (7)$$

the fixed point (E_s, φ_s) is determined for each value of F . In order to characterize the bifurcation point, it is not necessary to find the explicit expression for the stationary-state field.

It can be easily seen that $Y_s = -X_s/\delta$ is a tangent to the solution of Eqs. (5) at the origin when $E_s = 0$, while $Y_s = X_s/\kappa$ is an asymptote to the same solution curve when $E_s \rightarrow +\infty$. The particular case $X_s = 0$ corresponds to $E_s^2 = Y_s^2 = \delta/\kappa$.

To determine the stability of \mathcal{E}_s , we perform a perturbative analysis around \mathcal{E}_s . Let $\mathcal{E} = \mathcal{E}_s + \mathbf{e}$, where $\mathbf{e} = x + iy$, linearizing Eq. (2) in the neighborhood of \mathcal{E}_s . We have found the eigenvalues

$$\lambda_s = \alpha_s \pm \sqrt{\alpha_s^2 - \beta_s}, \quad (8)$$

where

$$\alpha_s = g_s - \gamma E_s^2 (1 + E_s^2)^{-2}, \quad (9)$$

$$\beta_s = g_s^2 - 2\gamma E_s^2 g_s (1 + E_s^2)^{-2} + 1.$$

The system's bifurcation point is reached when $\text{R}(\lambda_s) = 0$. To continue the analysis, we have considered the case $\lambda_s \in \mathbb{C}$.

There is only one physically acceptable solution for g_s for which $\alpha_s = 0$, namely,

$$g_b = \kappa(\sqrt{\sigma} - 1), \quad (10)$$

the adimensional gain at the bifurcation point, which here is $\sigma = \gamma/\kappa$. The field at the bifurcation point is defined by

$$E_b^2 = \sqrt{\sigma} - 1, \quad (11)$$

$$\varphi_b = -\cot^{-1} g_b,$$

while the frequency at the bifurcation point is $\beta_s = \Omega_b$,

so that,

$$\Omega_b^2 = 1 - g_b^2, \quad (12)$$

with $0 < |g_b| \leq 1$. This is the condition for \mathcal{E}_s to be a bifurcation point.

Given κ and γ , we call F_b the driving force needed to bring the system to the bifurcation point. From Eqs. (4) and (11), we get

$$F_b^2 = [\kappa^2(\sqrt{\sigma} - 1)^2 + 1](\sqrt{\sigma} - 1). \quad (13)$$

If $F < F_b$, the solution for \mathcal{E}_s is unstable, bringing the system to a limit-cycle solution. Instead of this, if $F > F_b$, \mathcal{E}_s is a fixed-point stable solution. From this we can see that F is what determines the stability of the stationary state, its value depending on the parameters κ and γ .

The frequency shift near the bifurcation point can be easily analyzed by writing Eq. (8) in terms of g_s ,

$$\lambda_s = g_s - f(g_s) \pm i\Omega_s, \quad (14)$$

real being Ω_s , and

$$f(g_s) = \sqrt{1 - \Omega_s^2}, \quad (15)$$

or

$$f(g_s) = \frac{1}{\gamma}(\delta - g_s)(\kappa + g_s). \quad (16)$$

The function f reaches its maximum for $g_{s,m} = \frac{1}{2}(\delta - \kappa)$ where $f(g_{s,m}) = \gamma/4$, and $E_{s,m} = 1$.

The system will reach a limit-cycle regime for $g_s > f(g_s)$, where $g_b < g_s \leq \delta$ (or, $0 < \Delta g \leq \sqrt{\sigma}g_b$, with $\Delta g = g_s - g_b$); it presents a fixed-point stable solution for $g_s < f(g_s)$, with $0 \leq g_s < g_b$.

In the limit-cycle regime, two different cases are being considered (see Fig. 1) as follows.

(i) $g_{s,m} < g_b \leq \delta$ ($1 \leq \sigma < 4$). From Fig. 1(a) and Eqs. (15) and (16), it is apparent that, as the system is driven apart from the bifurcation point, Ω_s increases, that is, decreasing F from F_b , i.e., increasing Δg , as can be seen by solving Eqs. (5)–(7) for different F values.

(ii) $g_b < g_{s,m}$ ($\sigma > 4$). From Fig. 1(b) and Eqs. (15) and (16), four cases have to be considered. (a) If $g_b < g_s < g_{s,m}$, then Ω_s decreases as the system is driven apart from the bifurcation point with $\Delta g > 0$. (b) If $g_{s,m} < g_s \leq \delta$, then Ω_s increases as the system is driven apart from the bifurcation point, with respect to the maximum $g_{s,m}$, increasing Δg . (c) If $g_s = g_{s,m}$, then the minimum frequency is obtained, namely, $\Omega_{s,m} = \sqrt{1 - (\gamma/4)^2}$. Finally, (d) if $g_b = g_{s,m}$ ($\sigma = 4$), then the solution is $E_{s,m} = 1$ being a zero-frequency bifurcation point. In its vicinity, the limit-cycle solutions are homoclinic orbits.

IV. STOCHASTIC MODEL

We proceed now to include temporal stochastic fluctuations of the relevant dynamical parameters of the system. We consider both amplitude and frequency fluctuations in the injected coherent field and the frequency of the laser itself.

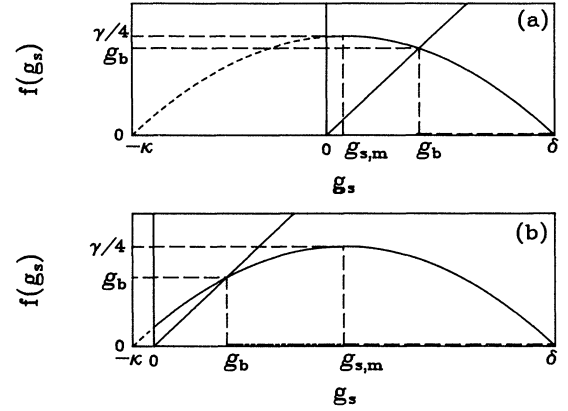


FIG. 1. $f(g_s)$ vs g_s . $f(g_s)$ is given by Eq. (15), g_s is the adimensional stationary net gain. The long-dashed line in the abscissa axis in (a) and (b) displays possible g_s values for which the dynamical regime is a limit cycle, where the Ω_s increases with an increase of g_s from the value g_b (a) or $g_{s,m}$ (b), see Eq. (15). The double dot-dashed line in the (b) abscissa axis displays the values of g_s to which the regime is a limit cycle. The Ω_s decreases when increasing g_s from g_b . The unfolding parameter, $\mu = g_s - f(g_s)$, defines g_b ($\mu = 0$) and the stability of the system at either side of g_b .

The detuning and the amplitude of the injected field have well-defined temporal mean values; we call these values

$$\langle \Delta_\nu(t) \rangle = \Delta_\nu, \quad (17)$$

$$\langle E_I(t) \rangle = E_I.$$

In the case of nonzero detuning, the scaling $\tau = \Delta_\nu t$, as before, leads to

$$\partial\tau\mathcal{E} = \left(\frac{i\Delta_\nu(\tau)}{\Delta_\nu} + g(E) \right) \mathcal{E} + \frac{\Delta_c\sqrt{T}}{\Delta_\nu} E_I(\tau). \quad (18)$$

Fluctuations can be expressed as

$$\frac{\Delta_\nu(\tau)}{\Delta_\nu} = 1 + u_3(\tau), \quad (19)$$

$$\frac{\Delta_c\sqrt{T}}{\Delta_\nu} E_I(\tau) = F + u_4(\tau),$$

where u_3 and u_4 are random functions with zero mean values and nonzero self-correlation functions.

The stochastic differential equation is, therefore,

$$\partial\tau\mathcal{E} = [i + g(E)]\mathcal{E} + F + iu_3\mathcal{E} + u_4. \quad (20)$$

In the case of white noise, the self-correlation functions are

$$\langle u_j(\tau)u_j(\tau') \rangle = D_j \delta(\tau - \tau') \quad (21)$$

for $j = 3, 4$; and $D_3 = \epsilon_3/\Delta_\nu^2$ and $D_4 = \Delta_c^2 T \epsilon_4/\Delta_\nu^2$, ϵ_3 and ϵ_4 being the fluctuation intensities in frequency and amplitude, respectively.

If the random variables are representatives of Ornstein-

Uhlenbeck processes, with zero mean value, then the correlations are

$$\langle u_i(\tau)u_j(\tau') \rangle = \delta_{ij} \frac{D_i \alpha_i}{2} \exp(-\alpha_i |\tau - \tau'|), \quad (22)$$

where α_i^{-1} is the correlation time of the i th process, and D_i its diffusion constant.

This kind of stochastic process is solved using Langevin's differential equations

$$\dot{u}_j(\tau) = -\alpha_j u_j(\tau) + \zeta_j(\tau), \quad (23)$$

where $\{\zeta_j(\tau)\}$ are uncorrelated white noises whose intensities are $\epsilon_j = D_j \alpha_j^2$.

If noises are absent (i.e., each $\epsilon_j = 0$), then Eqs. (18) and (23) have the solution $\mathcal{E} = \mathcal{E}_s$ and $u_j = 0$. The system presents a bifurcation at $\mathcal{E} = \mathcal{E}_b = X_b + iY_b$ with $u_j = 0$.

Around the bifurcation point, indicating $u_1 = X - X_b$ and $u_2 = Y - Y_b$, the stochastic differential equation for

a first-order expansion is

$$\partial_\tau \mathbf{u} = L_b \mathbf{u} + \mathbf{N}(\mathbf{u}) + \mathbf{Z}(\tau), \quad (24)$$

where $\mathbf{u} = u_i \mathbf{e}^i$, \mathbf{e}^i being the vectors of canonical base in \mathbb{C}^4 . (As a rule, repeated index implies summations, if crossed.)

The linear operator L_b in Eq. (24) is

$$L_b = \begin{pmatrix} A_b & C_b - 1 & -Y_b & 0 \\ C_b + 1 & B_b & X_b & 0 \\ 0 & 0 & -\alpha_3 & 0 \\ 0 & 0 & 0 & -\alpha_4 \end{pmatrix}, \quad (25)$$

with

$$\begin{aligned} A_b &= g_b - 2\kappa X_b^2, \\ B_b &= g_b - 2\kappa Y_b^2, \\ C_b &= -2\kappa X_b Y_b. \end{aligned}$$

The nonlinear operator is

$$\begin{aligned} \mathbf{N}(\mathbf{u}) &= \left\{ -u_2 u_3 + \sum_{n=1}^{+\infty} \left[\frac{X_b}{(n+1)!} \mathcal{D}^{(n+1)}(u_1, u_2) + \frac{u_1}{n!} \mathcal{D}^{(n)}(u_1, u_2) \right] \right\} \mathbf{e}^1 \\ &+ \left\{ u_1 u_3 + \sum_{n=1}^{+\infty} \left[\frac{Y_b}{(n+1)!} \mathcal{D}^{(n+1)}(u_1, u_2) + \frac{u_2}{n!} \mathcal{D}^{(n)}(u_1, u_2) \right] \right\} \mathbf{e}^2, \end{aligned} \quad (26)$$

where

$$\mathcal{D}^{(j)}(u_1, u_2) = \left(u_1 \frac{\partial}{\partial X} + u_2 \frac{\partial}{\partial Y} \right)^{(j)} g(X, Y) \Big|_{(X_b, Y_b)}.$$

Finally, the noise term is

$$\mathbf{Z}(\tau) = \zeta_i(\tau) \mathbf{e}^i \quad (i = 3, 4). \quad (27)$$

Let $\{\chi^i\}$ be the eigenvector base in \mathbb{C}^4 which diagonalizes L_b , i.e.,

$$L_b \chi^i = \lambda_i \chi^i. \quad (28)$$

The corresponding eigenvalues are

$$\begin{aligned} \lambda_{1,2} &= \pm i \Omega_b, \\ \lambda_j &= -\alpha_j \quad (j = 3, 4). \end{aligned} \quad (29)$$

In terms of the canonical base, χ^j are expressed as

$$\chi^j = \chi_k^j \mathbf{e}^k. \quad (30)$$

Next we present the nonzero coefficients χ^j related to the change of base,

$$\begin{aligned} \chi_1^1 &= \chi_1^2 = \chi_3^3 = \chi_4^4 = 1, \\ \chi_2^1 &= \overline{\chi_2^2} = -\frac{A_b - i\Omega_b}{C_b - 1}, \\ \chi_1^3 &= \frac{\alpha_3 Y_b}{\Omega_b^2 + \alpha_3^2}, \end{aligned}$$

$$\begin{aligned} \chi_2^3 &= -\frac{g_b(g_b - \alpha_3) + 1}{\Omega_b^2 + \alpha_3^2} Y_b, \\ \chi_1^4 &= \frac{B_b + \alpha_4}{\Omega_b^2 + \alpha_4^2}, \\ \chi_2^4 &= \frac{C_b + 1}{\Omega_b^2 + \alpha_4^2}. \end{aligned}$$

We can see that $\chi^1 = \overline{\chi^2}$. Lastly, we present the corresponding coefficients e_m^l for its inverse transformation,

$$\begin{aligned} e_1^1 &= \overline{e_2^1} = \frac{A_b + i\Omega_b}{2i\Omega_b}, \\ e_1^2 &= \overline{e_2^2} = \frac{C_b - 1}{2i\Omega_b}, \\ e_1^j &= \overline{e_2^j} = -(\chi_1^j e_1^1 + \chi_2^j e_1^2) \quad (j = 3, 4), \\ e_3^3 &= e_4^4 = 1. \end{aligned}$$

V. STOCHASTIC NORMAL FORM

In the neighborhood of the bifurcation point, it is always possible to make a nonlinear transformation of variables, which allows us to separate the resonances of the original stochastic differential equation [18, 19].

In the limit of very low-intensity white noise, the resonant contributions are mainly due to deterministic causes. When colored noise is included, the resonant contributions appear to be modified.

Modeling with colored noise allows us to describe both

effects, as white noise is reached as a particular color case. The stochastic normal form equation, together with a nonlinear change of variables, allows us to evaluate in a simple way [11] correlation function and higher moments and, as a consequence, the dominant spectral contributions too. Through the coefficients of the nonlinear transformation it is possible to obtain the intensity of the resonant peaks of the spectrum. The widths of the resonances are closely related to the inverse of the noise correlation time.

In Eq. (20), the presence of \mathbf{u}_4 breaks up the phase invariance symmetry, even when $F = 0$, and is responsible for the appearance of the stochastic resonances.

For the noise-free case, if $\mathbf{w} = \{w_j; j = 1, \dots, 4\}$ are the new variables, the original variables \mathbf{u} can be cast into the \mathbf{w} as

$$\mathbf{u} = \sum_{r(\geq 1)} \mathbf{u}^{[r]}(\mathbf{w}) = \sum_{r(\geq 1)} U_j^{j_1 \dots j_r} w_{j_1} \dots w_{j_r} \chi^j \quad (j_1 \leq \dots \leq j_r), \quad (31)$$

where the $\mathbf{u}^{[r]}$ are the terms at order r in $\{w_j\}$.

We want the differential equation (in the noise-free case) to be in the new variables

$$\partial_\tau w_j = \sum_{r(\geq 1)} F_j^{[r]}(\mathbf{w}). \quad (32)$$

Then, for example, for the first order ($r = 1$)

$$\mathbf{u}^{[1]} = w_j \chi^j \quad (33)$$

and

$$\mathbf{N}^{[3]}(\mathbf{w}) = \left\{ A_j^{j_1 j_2 j_3} u_{j_1}^{[1]} u_{j_2}^{[1]} u_{j_3}^{[1]} + A_j^{j_1 j_2} [u_{j_1}^{[1]} u_{j_2}^{[2]} + \mathcal{P}(j_1, j_2)] \right\} e^j \quad (j_1 \leq j_2 \leq j_3), \quad (40)$$

or, in the new variables,

$$\mathbf{N}^{[3]}(\mathbf{w}) = B_k^{k_1 k_2 k_3} w_{k_1} w_{k_2} w_{k_3} \chi^k \quad (k_1 \leq k_2 \leq k_3), \quad (41)$$

where

$$B_k^{k_1 k_2 k_3} = \left\{ \chi_{j_1}^{k_1} \chi_{j_2}^{k_2} \chi_{j_3}^{k_3} A_j^{j_1 j_2 j_3} + \chi_{j_1}^{k_1} \chi_{j_2}^l U_l^{k_2 k_3} [A_j^{j_1 j_2} + \mathcal{P}(j_1, j_2)] + \mathcal{P}(k_1, k_2, k_3) \right\} e_j^k, \quad (42)$$

where $\mathcal{P}(k_1, k_2, k_3)$ now indicates all permutations without repetition of the precedent terms in the sum.

The nonlinear change of variables, up to the second order, is

$$u_j = (w_i + w_{i_1} w_{i_2} U_i^{i_1 i_2} + \dots) \chi_j^i, \quad (43)$$

while the deterministic normal form is [19]

$$\partial_\tau w_j = w_j f_j(|w_1|^2), \quad (44)$$

with

$$f_1 = \bar{f}_2 = i \Omega_b + B_1^{112} |w_1|^2 + \mathcal{O}(|w_1|^4), \quad (45)$$

$$f_j = -\alpha_j + B_j^{12j} |w_1|^2 + \mathcal{O}(|w_1|^4) \quad (j = 3, 4).$$

$$F_j^{[1]} = \lambda_j w_j \quad (34)$$

are obtained.

For $r = 2$ (second order), the nonlinear part of the stochastic differential equation [see Eq. (26)], can be written as

$$\mathbf{N}^{[2]}(\mathbf{w}) = A_j^{j_1 j_2} u_{j_1}^{[1]} u_{j_2}^{[1]} e^j \quad (j_1 \leq j_2). \quad (35)$$

This equation expressed in the new base $\{\chi^k\}$ is

$$\mathbf{N}^{[2]}(\mathbf{w}) = B_k^{k_1 k_2} w_{k_1} w_{k_2} \chi^k \quad (k_1 \leq k_2), \quad (36)$$

where

$$B_k^{k_1 k_2} = \chi_{j_1}^{k_1} \chi_{j_2}^{k_2} e_j^k A_j^{j_1 j_2} + \mathcal{P}(k_1, k_2), \quad (37)$$

as can be demonstrated by straightforward algebra. $\mathcal{P}(k_1, k_2)$ indicates permutation without repetition of the precedent term.

If we ask for

$$F_j^{[2]} \equiv 0, \quad (38)$$

in the differential equation (32), then the second-order resonances are eliminated.

The coefficient of $\mathbf{u}^{[2]}$ in terms of \mathbf{w} is [19]

$$U_k^{k_1 k_2} = \left(\sum_i r_i \lambda_i - \lambda_k \right)^{-1} B_k^{k_1 k_2}, \quad (39)$$

where r_i is the order of the term of w_i in $u_k^{[r]}$.

For the third order, the nonlinear terms in the stochastic differential equation are

The noise terms, expressed on the base $\{\chi^i\}$, are

$$\mathbf{Z}(\tau) = \eta_i(\tau) \chi^i, \quad (46)$$

where

$$\eta_i(\tau) = \zeta_k e_i^k \quad (k = 3, 4). \quad (47)$$

Thus the stochastic normal form equation is

$$\partial_\tau w_j = w_j f_j(|w_1|^2) + \eta_j(\tau), \quad (48)$$

where $\langle \eta_i(\tau) \rangle$ are the white noises with zero mean values, and correlation functions

$$\langle \eta_i(\tau) \eta_j(\tau') \rangle = Q_{ij} \delta(\tau - \tau'), \quad (49)$$

and the noise intensity is

$$Q_{il} = e_i^k e_j^k \epsilon_k \quad (k = 3, 4). \quad (50)$$

It is clear that the stochastic dynamics will be governed by slow variables or critical modes ($w_1, w_2 = \bar{w}_1$), associated to complex-conjugate eigenvalues, and by fast variables or noncritical modes (w_3, w_4), associated to the noise terms. Fast variables have correlation times equal to α_j^{-1} , to first order in the variables of the stochastic normal form.

The stochastic dynamics in the neighborhood of the bifurcation point can now be described by introducing an unfolding parameter μ , which allows fixed-point or limit-cycle stable solutions to be reached when $\mu \simeq 0$. The stochastic normal form for critical modes, in the neighborhood of the bifurcation point, is

$$\partial_\tau w_1 = (\mu + i \Omega_b) w_1 + B_1^{112} |w_1|^2 w_1 + \eta_1(\tau), \quad (51)$$

where the coefficient B_1^{112} will be a function of σ, Ω_b .

The unfolding parameter $\mu = \text{Re } \lambda_s$ can be interpreted in terms of physical parameters. If the working point of the system is such that

$$g_s = g_b + \Delta g, \quad (52)$$

$$\Omega_s = \Omega_b + \Delta \Omega,$$

with $\Delta g \ll g_b < 1$, and $\Delta \Omega \ll \Omega_b < 1$ then, to a first-order expansion of Eq. (14) around g_b ,

$$\mu = \frac{2\Delta g}{\sqrt{\sigma}} + \mathcal{O}(\Delta^2 g), \quad (53)$$

while, in terms of the shift $\Delta \Omega$,

$$\Delta g = -\frac{\Omega_b \Delta \Omega}{g_b(1 - 2/\sqrt{\sigma})}, \quad (54)$$

to first order in $\Delta \Omega$. Equation (54) allows us to describe the shift in frequency only in the neighborhood of the bifurcation point [this excludes the case ii(d) of Sec. II].

Since $\text{Re}(B_1^{112}) < 0$, it is possible to reach either a fixed-point stable solution for $\mu < 0$, or a limit-cycle stable solution for $\mu > 0$ (see Fig. 2). The limit-cycle radius in this case will be $R = \sqrt{-\mu/\text{Re}(B_1^{112})}$, and its frequency $\Omega_s \simeq \Omega_b - \mu \text{Im}(B_1^{112})/\text{Re}(B_1^{112})$.

Since the electric field is $\mathcal{E} = \mathcal{E}_b + (u_1 + i u_2)$, the cross-correlation function $\langle E(\tau) \bar{E}(\tau') \rangle$ should be a resonant contribution of moments, and cross-correlation functions of the form

$$C_j^m(\tau - \tau') = \langle w_j^m(\tau) \overline{w_j^m(\tau')} \rangle \quad (j = 1, 2). \quad (55)$$

If $w_1 \sim R e^{i \Omega_s \tau}$, then

$$C_j^m(\tau - \tau') \sim R^{2m} \exp[i(-1)^{j+1} m \Omega_s(\tau - \tau')], \quad (56)$$

where the resonances, multiples of Ω_s , become apparent.

VI. NUMERICAL SIMULATION

Numerical integration of the stochastic differential equations (20) and (23) was done by conventional procedures as described, for example, in Ref. [20]. After elim-

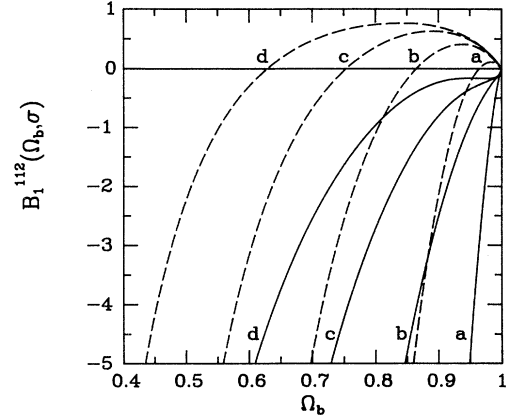


FIG. 2. Cubic coefficient of the stochastic normal form [Eq. (42)] as a function of Ω_b . Parameter $\sigma = \gamma/\kappa$ is (a) 1.2; (b) 1.6; (c) 2.0; (d) 2.4. Dashed line is $\text{Im}(B_1^{112})$; full line is $\text{Re}(B_1^{112})$. Note that $\text{Re}(B_1^{112}) < 0$, in all cases.

inating the transients, the electric field values of each of the 200 simultaneous realizations simulating the stochastic process were used to evaluate the Fourier coefficients for each stage in the integration, thus getting the power spectral density through the Wiener-Khinchine theorem relations. All cases have been solved with similar numerical parameters. The integration adimensional time pitch used was 10^{-3} . The Fourier coefficients are taken from 512 samples, after an inspection of the precision we looked for.

Figure 3 displays the power spectral density for the following set of parameters: $\gamma = 3, \kappa = 2, D_3 = D_4 = 10^{-3}$. In this case, from Eqs. (12) and (13), the evaluated $F_b = 0.519$, and $\Omega_b = 0.893$. In Fig. 3(a) $F = 0.35$ and

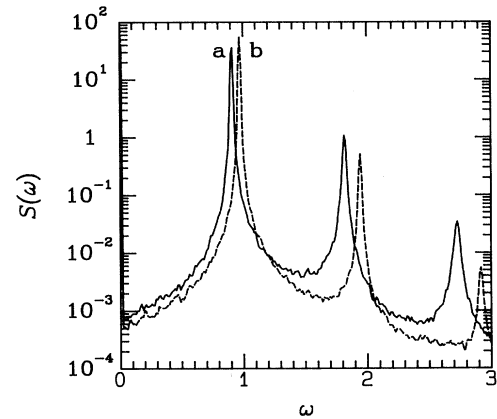


FIG. 3. Power spectral density vs adimensional ω with $F < F_b$ for the following parameters: $\gamma = 3, \kappa = 2, D_3 = D_4 = 10^{-3}$. The evaluated $F_b = 0.519$, and $\Omega_b = 0.893$. In (a) $F = 0.35$ and in (b) $F = 0.20$. In both cases only white noise was present. The main resonant contribution at frequency near Ω_s and its harmonics up to the second order can be seen. Note that when F is nearer to the F_b the spectral background near the central frequency is greater.

in Fig. 3(b) $F = 0.20$, instead.

Only white noise was generated in both cases, and they correspond to $F < F_b$. The main resonant contribution can be seen at a frequency near Ω_b , and its harmonics up to the second order. The frequency shifts in the spectrum are due to the change in F . The simulations correspond, in Fig. 1(a), to the case where Ω increases when F decreases with respect to F_b .

Figure 4 displays the power spectral density corresponding to two cases where the dynamical variable u_4 undergoes a white-noise process, and the u_3 a colored-noise one. In the spectrum of Fig. 4(a) the value for the inverse of correlation time is $\alpha_3 = 0.1$; and in the spectrum of Fig. 4(b), this takes the value $\alpha_3 = 2.0 \times 10^{-3}$, instead. In both cases $\alpha_4 = 10$, $\epsilon_3 = \epsilon_4 = 10^{-3}$. The laser parameters are $\gamma = 3$, $\kappa = 2$, and $F = 0.475$.

A frequency shift for the main resonant peaks becomes apparent, together with a broadening of the resonances when the correlation time for the colored noise is increased. Further increase in this parameter will wash all higher resonant contributions out of the spectrum.

Figure 5 shows the power spectral density corresponding to two cases where the dynamical variable u_3 undergoes a white-noise process, and the u_4 a colored-noise one. In the spectrum of Fig. 5(a) the value for the inverse of correlation time is $\alpha_4 = 0.1$; and in the spectrum of Fig. 5(b) this takes the value $\alpha_4 = 2.0 \times 10^{-3}$. In both cases $\alpha_3 = 10$, $\epsilon_3 = \epsilon_4 = 10^{-3}$. The laser parameters are $\gamma = 3$, $\kappa = 2$, and $F = 0.475$.

As is evident by comparison with Fig. 4, the resonances are still visible even when the correlation time for the colored noise in the amplitude is comparable to the colored noise in the frequency as displayed in Fig. 4. This result

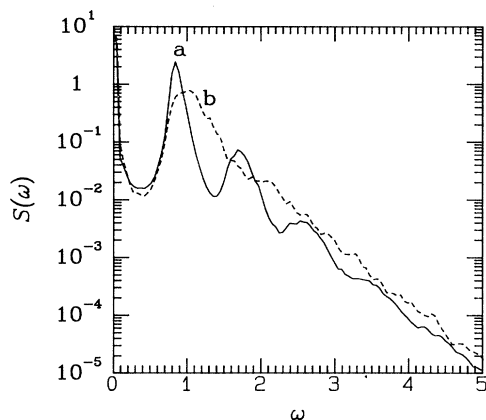


FIG. 4. Power spectral density corresponding to two cases where the dynamical variable u_4 undergoes a white-noise process, and u_3 a colored-noise one. The case (a) corresponds to a value for the inverse of correlation time $\alpha_3 = 0.1$; and (b) for $\alpha_3 = 2.0 \times 10^{-3}$. In both cases $\alpha_4 = 10$, $\epsilon_3 = \epsilon_4 = 10^{-3}$. The laser parameters are $\gamma = 3$, $\kappa = 2$, and $F = 0.475$. A frequency shift for the main resonant contribution becomes apparent, together with a broadening of the resonant peaks when the correlation time for the colored noise is increased. Further increase in this parameter will wash all higher resonant contributions out of the spectrum.

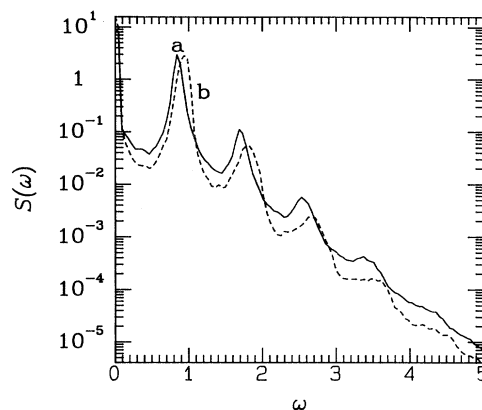


FIG. 5. Power spectral density corresponding to two cases where the dynamical variable u_3 undergoes a white noise, and u_4 a colored-noise one. (a) corresponds to a value for the inverse of correlation time $\alpha_4 = 0.1$; and (b), $\alpha_4 = 2.0 \times 10^{-3}$. In both cases $\alpha_3 = 10$, $\epsilon_3 = \epsilon_4 = 10^{-3}$. The laser parameters are $\gamma = 3$, $\kappa = 2$, and $F = 0.475$. Note that the resonances are still visible compared with Fig. 4.

evidences the importance of the phase as a dynamical variable.

In the case $F > F_b$, the spectra show the normal appearance of an injection-locked laser, consisting of a very narrow central peak on a noisy background. In the case of colored noise, this background is larger than in the white-noise case.

As concluding remarks on the results shown here, we can say that fluctuations in the injected-signal intensity increase the linewidths if the fluctuations are memory processes; a shift in the main resonant contribution is also apparent. In the case of fluctuations of the laser frequencies, instead, if they are memory process, then not only is a broadening evident, but a severe change in the dynamics of the system appears to take place too, displayed by a featureless line shape. The numerical solution is very flexible so that other problems of the kind can be analyzed in detail.

VII. SUMMARY

In this paper a Hopf bifurcation at the phase-locking point of an externally injected laser is studied in detail. Such a bifurcation point can only be accessed when a certain detuning between the laser and the external coherent signal is present. This is important in cases whenever the lasers to be locked in phase are of different nature than the generator of the coherent signal.

Our results can be applied to additive, multiplicative white or colored noise in unidirectional cavities as well. A model for bidirectional cavities is straightforward, and their consequences are presently under study.

Our analysis takes full account of two problems that are generally neglected when statistical physics is concerned. First, it can be generalized to cases where adiabatic elimination procedure is not possible for some dynamical variable of the problem. Secondly, the saturation

of the gain is expressed in the more general form. This saturation of the gain is, in fact, the mechanism responsible for the oscillatory behavior of the dynamical system, together with the evolution of the phase.

As can be seen from the results presented here, the bifurcation arises as a consequence of driving this type of nonlinear system to the stationary state by an external force. Near the phase-locking point, the output of the laser will oscillate with a frequency related to the external signal and to the parameters of the laser, and its harmonics.

The introduction of white noise (additive and multiplicative to the parameters) results in the appearance of narrow resonant peaks on a noisy line shape, while for the colored Ornstein-Uhlenbeck processes, a shift and widening of the resonances can eventually wipe out any feature in the spectrum. This is interpreted as a very long-term memory; thus the signal necessary to lock the system in phase should eventually become very large to be of any

practical interest. As pointed out in the Introduction, such memory processes can, for example, be introduced by the same system, if a retarded path is provided for the field.

The numerical results presented here thoroughly agree with the results expected from an analysis of the stochastic normal form of this problem which was found to correspond to a generalization of similar problems in laser dynamics.

ACKNOWLEDGMENTS

The authors wish to acknowledge Professor E. Tirapegui and Professor J. R. Tredicce for their kind encouragement during the earlier stages of this work. Work supported by Grant No. PID 3-155200-88 granted by Consejo Nacional de Investigaciones Científicas y Técnicas de la Republica Argentina.

-
- * Author to whom all correspondence should be addressed.
- [1] A. E. Siegman, *Laser* (University Science Books, Mill Valley, CA, 1986), and references therein.
 - [2] S. A. Shakir and W. W. Chow, *Opt. Lett.* **9**, 202 (1984).
 - [3] H. F. Ranea-Sandoval, M. C. Von Reichenbach, R. Rodrigue, and F. A. Schaposnik, *Opt. Commun.* **49**, 39 (1986).
 - [4] W. W. Chow, J. Gea Banacloche, L. M. Pedrotti, V. E. Sanders, W. Schleich, and M. O. Scully, *Rev. Mod. Phys.* **57**, 61 (1985).
 - [5] J. R. Tredicce, T. F. Arecchi, G. L. Lippi, and G. P. Puccioni, *J. Opt. Soc. Am.* **2**, 173 (1985).
 - [6] J. R. Tredicce and N. B. Abraham, in *Proceedings of the International School on Laser and Quantum Optics*, edited by L. M. Narducci, E. J. Quel, and J. R. Tredicce, CIF Series Vol. 13 (World Scientific, Singapore, 1990).
 - [7] T. Kapitaniak, *Phys. Lett. A* **116**, 251 (1986).
 - [8] Hu Gang and Lu Zhi-heng, *Phys. Rev. A* **44**, 8027 (1991).
 - [9] B. Dorizzi, B. Grammaticos, M. Le Berre, Y. Pomeau, E. Ressayre, and A. Tallet, *Phys. Rev. A* **35**, 328 (1987).
 - [10] M. Le Berre, E. Ressayre, A. Tallet, and Y. Pomeau, *Phys. Rev. A* **41**, 6635 (1990).
 - [11] R. C. Buceta and E. Tirapegui, in *Instabilities and Nonequilibrium Structures III*, edited by E. Tirapegui and W. Zeller (Kluwer, Dordrecht, 1991).
 - [12] A. Shenze and H. Brand, *Opt. Commun.* **27**, 485 (1978).
 - [13] E. Peacock-Lopez, F. J. de la Rubia, B. J. West, and K. Lindenberg, *Phys. Rev. A* **39**, 4026 (1989).
 - [14] F. C. Cheng and L. Mandel, *J. Opt. Soc. Am. B* **8**, 1681 (1991).
 - [15] J. O'Gorman, B. J. Hawdon, J. Hegarty, and D. M. Hefernan, *J. Appl. Phys.* **66**, 1 (1988).
 - [16] M. Aguado and M. San Miguel, *Phys. Rev. A* **37**, 450 (1988).
 - [17] M. Aguado, E. Hernández-García, and M. San Miguel, *Phys. Rev. A* **38**, 5670 (1988).
 - [18] J. Guckenheimer and P. Holmes, in *Nonlinear Oscillations, Dynamical Systems, and Bifurcations of Vector Fields*, edited by F. John, J. E. Marsden, and L. Sirovich, Applied Mathematical Sciences Vol. 42 (Springer-Verlag, Berlin, 1983).
 - [19] P. Couillet, C. Elphick, and E. Tirapegui, *Phys. Lett.* **111A**, 277 (1985).
 - [20] M. Sancho, M. San Miguel, S. L. Katz, and J. D. Gunton, *Phys. Rev. A* **26**, 1589 (1982).